Metals and Materials International (2018) 24:730–737
https://doi.org/10.1007/s12540-018-0097-4

Grain-Refined AZ92 Alloy with Superior Strength and Ductility

Jong Un Lee[1] · Sang-Hoon Kim[1] · Wan-Kuen Jo[2] · Won-Hwa Hong[3] · Woong Kim[2] · Jun Ho Bae[4] · Sung Hyuk Park[1]

Received: 29 August 2017 / Accepted: 7 January 2018 / Published online: 14 March 2018

Abstract

Grain-refined AZ92 (GR-AZ92) alloy with superior tensile properties is developed by adding 1 wt% Zn and a very small amount of SiC (0.17 wt%) to commercial AZ91 alloy for enhancing the solid-solution strengthening effect and refining the crystal grains, respectively. The homogenized GR-AZ92 alloy with an average grain size of 91 µm exhibits a tensile yield strength (TYS) of 125 MPa, ultimate tensile strength (UTS) of 281 MPa, and elongation of 12.1%, which are significantly higher than those of AZ91 alloy with a grain size of 420 µm (TYS of 94 MPa, UTS of 192 MPa, and elongation of 7.0%). The peak-aging time of GR-AZ92 alloy (8 h) is significantly shorter than that of AZ91 alloy (32 h) owing to a larger amount of grain boundaries in the former, which serve as nucleation sites of $Mg_{17}Al_{12}$ precipitates. A short-aging treatment for less than 1 h of the GR-AZ92 alloy causes an effective improvement in its strength without a significant reduction in its ductility. The 30-min-aged GR-AZ92 alloy has an excellent combination of strength and ductility, with a TYS of 142 MPa, UTS of 304 MPa, and elongation of 8.0%.

Keywords Metals · Casting · Aging · Grain refinement · Tensile test

1 Introduction

With the tightening regulations on the fuel efficiency and carbon dioxide emissions of vehicles, efforts are actively underway to reduce the weight of the vehicle body in order to conform to these regulations [1]. In this context, magnesium, which has the lowest density among commercially available structural metal materials, has been attracting increasing attention for application in the transportation industry. Cast Mg alloys have been applied to various automobile components such as seat frames, instrument panel structures, radiator supports, transmission cases, and engine blocks [1, 2]. Mg-9 wt% Al-1 wt% Zn (AZ91) alloy is known to have excellent castability and relatively superior mechanical properties and corrosion resistance to other cast Mg alloys; for this reason, more than 90% of cast Mg products are used in the form of AZ91 alloy [3]. However, because Mg alloys generally have lower strength than steels and Al alloys—which are the predominantly used metals in automobiles—it is imperative to improve the mechanical properties of Mg alloys to enable them to replace steel or Al components.

The strength of cast Mg alloys can be improved by the addition of rare earth (RE) elements [4–7] or reinforcements [8–12]. Zhang et al. [4] reported that the addition of Y-rich misch metal (Ymm) effectively improves the tensile yield strength (TYS) of cast AZ91 alloy and showed that AZ91-0.8Ymm (wt%) alloy exhibits excellent tensile properties, with a TYS of 160 MPa, ultimate tensile strength (UTS) of 272 MPa, and elongation of 11%. Furthermore, Wang et al. [5] demonstrated that cast AZ91 alloy with added 1.0 wt% Nd has considerably higher tensile properties (TYS of 120 MPa, UTS of 172 MPa, and elongation of 3.9%) than cast AZ91 alloy (TYS of 100 MPa, UTS of 161 MPa, and elongation of 3.2%). Cast AZ91 alloys containing these RE elements (e.g., Y, Nd, Ce, La, and Gd) exhibit superior tensile properties, with a TYS of 102–161 MPa, UTS of 152–272 MPa, and elongation of 3.1–14.0% [4–7]. However, the addition of these expensive RE elements to Mg

✉ Sung Hyuk Park
sh.park@knu.ac.kr

1 School of Materials Science and Engineering, Kyungpook National University, Daegu 41566, Republic of Korea

2 Department of Environmental Engineering, Kyungpook National University, Daegu 41566, Republic of Korea

3 School of Architecture, Kyungpook National University, Daegu 41566, Republic of Korea

4 Implementation Research Division, Korea Institute of Materials Science, Changwon 51508, Republic of Korea

alloys—whose material price is already higher than that of competitive material Al alloys—causes an increase in the cost of the final products; the consequential lower cost competitiveness of these products reduces their practical applicability. The addition of reinforcements such as silicon carbide (SiC), aluminum borate, and Cu particulates is also highly effective in improving the strength of the cast material [8–12]. Ho et al. [8] showed that the addition of 15 wt% SiC to AZ91 alloy improves the TYS and UTS of the cast alloy by 257 and 289 MPa, respectively. Zheng et al. [9] also developed a high-strength cast AZ91 alloy with a TYS of 266 MPa and UTS of 352 MPa through the addition of 30 wt% $Al_{18}B_4O_{33}$ whiskers. The strength of the cast AZ91 alloy can be improved by the addition of these reinforcements (TYS of 122–299 MPa and UTS of 152–385 MPa), but its tensile elongation decreases considerably owing to a loss of ductility by the addition of hard and/or brittle reinforcements (elongation of 0.7–1.38%) [8–12]. Such low elongation makes it difficult to use reinforced cast AZ91 alloy as a structural component that requires certain levels of ductility and toughness.

Therefore, in order to expand the application range of cast Mg alloys, it is necessary to improve both their strength and elongation without increasing the cost of the final products. This study attempted to develop RE-free Mg–Al–Zn alloy with superior tensile properties to commercial AZ91 alloy through multiple applications of various strengthening mechanisms. For this purpose, the Zn content of AZ91 alloy was optimized to enhance the solid-solution strengthening effect and the grain size was refined by adding a very small amount of SiC to achieve grain-boundary strengthening. A short-aging treatment was then performed to induce precipitation strengthening without a large reduction in ductility. The end product was a grain-refined AZ92 (GR-AZ92) alloy with excellent strength and ductility. This paper discusses the enhancement of the tensile properties of the alloy through Zn addition and grain refinement and the control of its tensile strength and elongation via a short-aging treatment.

2 Experimental Procedure

Cast ingots of Mg–9Al–0.2Mn alloys with different Zn contents—i.e., 1, 2, 3, and 4 wt% (hereafter referred to as AZ91, AZ92, AZ93, and AZ94, respectively)—were prepared by first melting them in an electric resistance furnace at 750 °C under an inert atmosphere containing a mixture of CO_2 and SF_6 gases, then holding the molten metal at 700 °C for 15 min to stabilize it, and finally pouring it into a steel mold preheated to 210 °C. A cast ingot of GR-AZ92 alloy was fabricated by adding a small amount (0.7 wt% melt) of Al-SiC master alloy (20 vol% SiC) to molten AZ92 at 750 °C during the casting process; the SiC particles (10 μm in size) included in the Al-SiC master alloy serve to enhance the heterogeneous nucleation of the primary Mg phase and refine the microstructure of the cast billet [13, 14]. All cast ingots were homogenized at 410 °C for 24 h and then water-quenched. For aging treatment, the homogenized AZ91, AZ92, and GR-AZ92 alloys were machined to rectangular samples with dimensions of $20\times20\times10$ mm^3; aging heat treatment was performed at 200 °C for up to 64 h.

The microstructures of the as-cast and homogenized samples were analyzed by optical microscopy (OM), and the average grain size of the homogenized samples was measured by averaging the values obtained from five OM images through the linear intercept method. The hardness of the homogenized and aged samples was measured using a Vickers microhardness tester with a load of 0.2 kgf and a dwell time of 10 s. All hardness values were determined by averaging values excluding the maximum and minimum values measured at 10 different positions for each sample. Tensile tests of the homogenized and aged samples were performed at room temperature by using an Instron 4206 universal testing machine with a strain rate of 1.0×10^{-3} s^{-1}. The tests were performed three times using dog-bone-shaped samples (gage section: Ø6 mm × 25 mm) by means of an extensometer, and the average values of these measurements were used in this study.

3 Results and Discussion

It has been reported that Zn in the solid-solution state causes a larger change in both the *a* and *c* lattice parameters of Mg than do Al, Cd, Ga, In, Li, Mn, Sc, and Sn at a given atom concentration [15, 16]; this means that Zn is a highly effective alloying element for solid-solution strengthening of Mg. Therefore, the strength of AZ91 alloy—which is a representative cast Mg alloy with good mechanical properties—can be improved by controlling the Zn content of the alloy. Figure 1a shows the equilibrium phase diagram for Mg–9Al–0.2Mn–xZn (x = 0–6 wt%), as calculated with PANDAT software. From the calculated phase diagram, it can be seen that the maximum solid solubility of Zn in Mg–9Al–0.2Mn alloy is 2.74 wt% at 402 °C. To verify the effect of Zn content on the mechanical properties of cast alloys, Mg–9Al–0.2Mn–xZn (x = 1–4 wt%) alloys were fabricated, and the tensile properties of the homogenized alloys were measured. Figure 1b shows the variations in the TYS, UTS, and elongation of the alloys with the Zn content. Both the strength and the elongation improve up to the addition of 2 wt% Zn, but the tensile properties, especially the UTS and the elongation, deteriorate when more than 3 wt% Zn is added. The higher strength and elongation of the AZ92 alloy than those of the AZ91 alloy are attributed to the additional

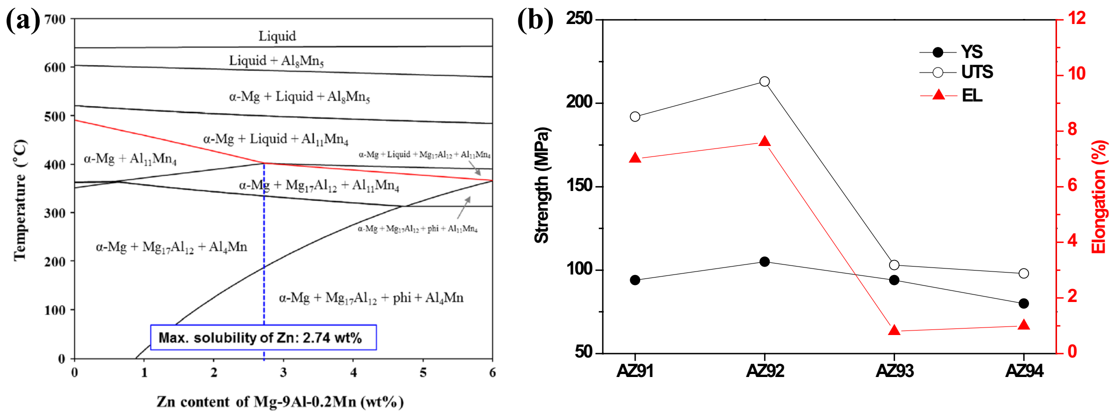

Fig. 1 **a** Equilibrium phase diagram for Mg–9Al–0.2Mn–xZn (x = 0–6 wt%), as calculated with PANDAT software. **b** Variation in tensile properties of homogenized AZ9x alloys with increase in Zn content. YS, UTS, and EL denote the yield strength, ultimate tensile strength, and elongation, respectively

effects of solid-solution strengthening and grain refinement induced by a higher Zn content. As the Zn content of the AZ93 and AZ94 alloys is higher than the maximum solubility of 2.74 wt%, internal microvoids are formed by local melting during homogenization heat treatment. Since these defects act as crack sources during plastic deformation, the alloys undergo premature fracture after yielding under tensile loading; this results in a drastic reduction in their UTS and ductility. Therefore, the AZ92 alloy with strength and elongation superior to those of commercial AZ91 alloy is selected, and the crystal grains of this alloy are made finer through the addition of a grain refiner to further improve the tensile properties.

Owing to the high growth restriction factor (GRF) of Zr and similar crystal structure to Mg, Zr has been considered as a highly effective grain refiner for Al-free Mg alloys such as pure Mg and Mg–Zn-based alloys [17, 18]. However, Zr is an ineffective grain refiner for Mg alloys containing Al, Si, and/or Mn, because the strong affinity of Zr with Al, Si, and Mn causes the formation of intermetallic compounds [19, 20]. Carbon inoculation is regarded as the most effective way to refine the grains of Mg–Al alloys, and it is commonly known that aluminum carbide plays an important role of a potent nucleant that promotes heterogeneous nucleation [21, 22]. Carbon can be introduced into the melt in various forms such as C_2Cl_6, Al_4C_3, $MgCO_3$, $MnCO_3$, and graphite powders [21–26]. One method of carbon inoculation is the use of SiC—which has been widely used as a reinforcement in Al- and Mg-based composites—as an effective grain refiner for Al-bearing Mg alloys [27–29]; it has a particularly remarkable grain refining effect when added to Mg–Al alloys containing less than 9 wt% Al [30]. When a large amount of SiC is added, the Si decomposed from the SiC particles reacts with Mg to give a Mg_2Si phase with "Chinese-script" morphology; this leads to a deterioration in the tensile properties of the cast material [30]. For example, a considerable amount of Mg_2Si and/or residual SiC particles are present in Mg–3Al–10SiC (wt%) [27] and AZ91-5SiC (wt%) [30] alloys. In the present study, to refine the grain size of the AZ92 alloy without the formation of the Mg_2Si phase, a very small amount of SiC (0.17 wt%) was added to the melt in the form of an Al–SiC master alloy.

Figure 2 shows the microstructures of the as-cast, homogenized, and peak-aged AZ91, AZ92, and GR-AZ92 alloys. In all the alloys, the dendrite structure and second phase formed during solidification nearly disappeared by the homogenization treatment, except for a small amount of the Al_8Mn_5 phase; the presence of thermally stable Al_8Mn_5 particles is consistent with previously reported results for homogenized Mg–7.63Al–0.38Zn–0.15Mn (wt%) [31], Mg–8.6Al–0.67Zn–0.22Mn (wt%) [32], and Mg–7.45Al–1.85Zn–0.15Mn (wt%) [33] alloys. The average grain size of the homogenized AZ92 alloy (420 µm) is smaller than that of the AZ91 alloy (494 µm), which means that slight grain refinement is caused by the additional 1 wt% Zn. The homogenized GR-AZ92 alloy has a much smaller grain size than the other alloys, and the addition of 0.17 wt% SiC to AZ92 alloy results in significant grain refinement from 420 to 91 µm. In addition, the AZ91 and AZ92 alloys without added SiC have large grain size distributions of ~ 200–1000 µm, whereas the GR-AZ92 alloy exhibits a relatively uniform grain structure. This is because the addition of SiC to the molten AZ92 alloy provides more nucleation sites that are present in the melt and restricts the grain growth, which leads to smaller, more, and equiaxed grains after solidification. After peak aging, two types of $Mg_{17}Al_{12}$ precipitates—i.e., discontinuous precipitates (DPs) and continuous precipitates (CPs)—were formed in all the alloys. The DPs with a lamellar structure of α-Mg and β-$Mg_{17}Al_{12}$ formed around the grain boundaries, and the

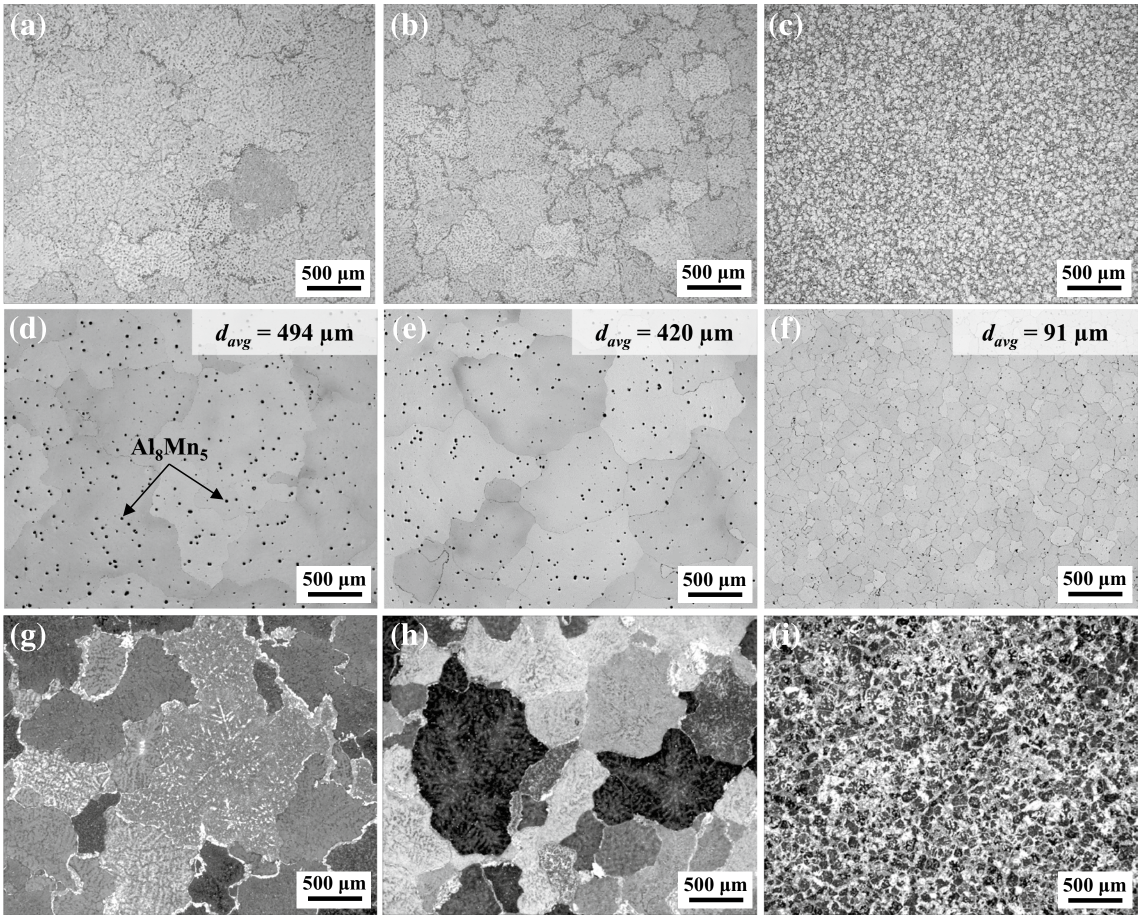

Fig. 2 Optical micrographs of **a**–**c** as-cast, **d**–**f** homogenized, and **g**–**i** peak-aged, **a**, **d**, **g** AZ91, **b**, **e**, **h** AZ92, and **c**, **f**, **i** grain-refined AZ92 alloys. d_{avg} denotes the average grain size

CPs with plate-type or lath-type morphology formed inside the crystal grains [34, 35]. The DPs are more homogeneously distributed in the GR-AZ92 alloy than the AZ91 and AZ92 alloys due to a larger area fraction of grain boundaries in the former. According to our previous study, the grain refinement increases the nucleation site of DPs, but does not affect their growth rate [36].

The age hardening curves of the homogenized AZ91, AZ92, and GR-AZ92 alloys are shown in Fig. 3, which reveals that the aged AZ92 alloy has higher hardness than the aged AZ91 alloy at a given aging time. Moreover, the difference in hardness in the peak-aged states of the AZ91 and AZ92 alloys (32 and 24 h, respectively), 7.5 Hv, is greater than that in the homogenized state, 3.4 Hv. This increase in peak hardness and decrease in peak-aging time in the AZ92 alloy compared to the AZ91 alloy are related to the variation in solid solubility of Al upon the addition of 1 wt% Zn [37, 38]. Since the solid solubility of Al in Mg decreases with increasing Zn content, more $Mg_{17}Al_{12}$ precipitates form during aging treatment with added Zn, resulting in increased peak hardness. In addition, the formation of more precipitates reduces the peak-aging time owing to the saturation of the nucleation sites of precipitates [36]. This

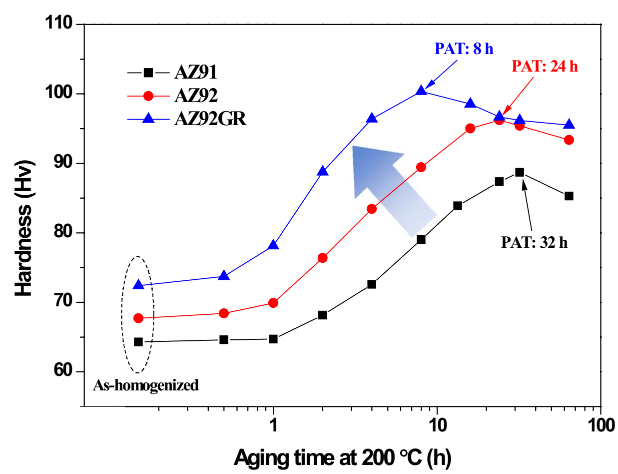

Fig. 3 Age hardening curves of AZ91, AZ92, and grain-refined AZ92 alloys. PAT denotes the peak-aging time

drastic reduction in the peak-aging time of the GR-AZ92 alloy is because the amount of grain boundaries, which serve as nucleation sites of the DP of the $Mg_{17}Al_{12}$ phase [39, 40], increases by grain refinement, leading to the promotion of precipitation behavior during aging. This agrees with the fact that the slope of the age hardening curve in the time range of 1–4 h, wherein the DP is mainly formed at the aging temperature of 200 °C [41], is larger for the GR-AZ92 alloy than for the AZ91 and AZ92 alloys (Fig. 3). These results demonstrate that the GR-AZ92 alloy with refined grains not only has higher hardness than the commercial AZ91 alloy in a homogenized state but also shows accelerated precipitation behavior during aging treatment, resulting in a shorter peak-aging time and a stronger precipitation strengthening effect.

The homogenized GR-AZ92 alloy with enhanced solid-solution and grain-boundary strengthening effects is subjected to aging treatment for improving its tensile strength further through the formation of precipitates. It is known that when peak-aging treatment is performed to improve the yield strength of cast Mg–Al alloys, the strength effectively increases because of the formation of precipitates, whereas the ductility decreases drastically owing to the excessive formation of brittle DPs along the grain boundaries and the reduction in the ductility of the matrix by the formation of numerous CPs in the grains [42, 43]. Furthermore, the reduction in elongation by the formation of brittle DPs can be more pronounced in grain-refined alloys because more DPs are formed at the grain boundaries during aging. Accordingly, to obtain a good combination of strength and ductility through aging treatment, the formation of excessive brittle DP phase should be prevented at the time a certain precipitate strengthening effect is induced through the formation of precipitates. For this purpose, the GR-AZ92 alloy is aged for a relatively short time less than 1 h (this under-aging treatment is referred to herein as a short-aging treatment); a peak-aging treatment is also performed for 8 h for comparison purposes. Figure 4 shows the tensile stress–strain curves of the homogenized, short-aged, and peak-aged GR-AZ92 samples, along with the curves of the homogenized AZ91 and AZ92 samples; the tensile properties of the samples are listed in Table 1. The homogenized GR-AZ92 sample exhibits significantly superior tensile properties to the other homogenized samples. The TYS, UTS, and elongation of the GR-AZ92 sample are ~ 33, ~ 46, and ~ 76% higher, respectively, than those of the AZ91 sample; the increase in strength is attributed to the combined effects of the solid-solution strengthening caused by Zn addition and the grain-boundary strengthening caused by grain refinement. In particular, it is known that the mechanical properties of Mg alloys are greatly influenced by the grain size [44, 45], which is confirmed by the fact that the value of the Hall–Petch coefficient of Mg alloys is approximately four times that of Al alloys [45, 46]. Therefore, grain refinement is a much more effective way to improve the strength of Mg alloys. The homogenized AZ91 and AZ92 samples have similar elongations of 7.0 and 7.6%, respectively, whereas the homogenized GR-AZ92 sample has a

Table 1 Tensile properties of homogenized and aged AZ91, AZ92, and grain-refined AZ92 (GR-AZ92) alloys

Alloy	Heat-treated state	YS (MPa)	UTS (MPa)	EL (%)
AZ91	Homogenized	94	192	7.0
AZ92	Homogenized	105	213	7.6
GR-AZ92	Homogenized	125	281	12.1
	Aged for 10 min	130	297	9.6
	Aged for 30 min	142	302	8.0
	Aged for 60 min	145	304	6.4
	Peak-aged for 8 h	161	256	2.5

YS, UTS, and EL denote the tensile yield strength, ultimate tensile strength, and elongation, respectively

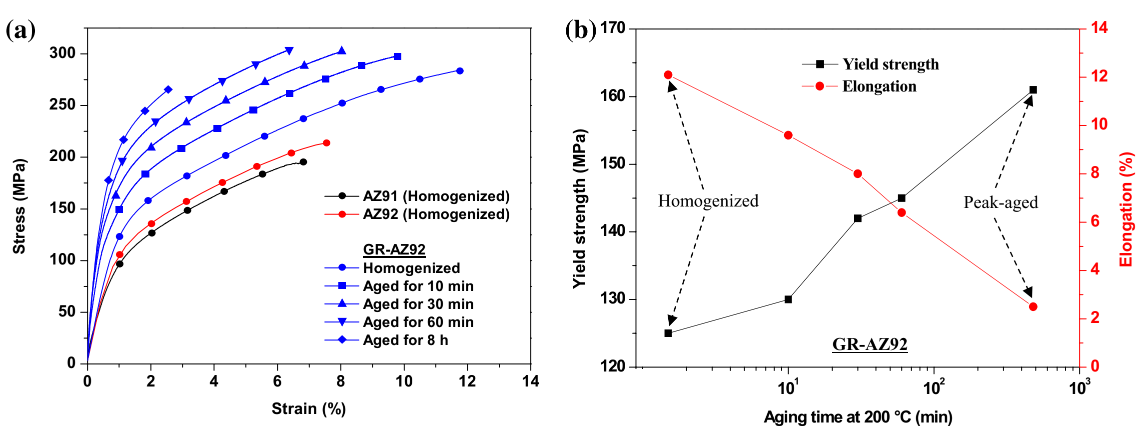

Fig. 4 **a** Tensile stress–strain curves of homogenized and aged alloys. **b** Variation in yield strength and elongation of grain-refined AZ92 alloy with aging time

much higher elongation (12.1%) than these two samples. As the twinning stress increases with a decrease in grain size, the formation of twins—which act as crack sources—during tensile deformation is suppressed in the GR-AZ92 sample with smaller grains; this results in an increase in its ductility [47, 48]. As the aging time increases up to 1 h, the TYS of the GR-AZ92 samples increases gradually from 125 to 145 MPa whereas its elongation decreases gradually from 12.1 to 6.4% (Fig. 4a, Table 1). The 8-h-peak-aged GR-AZ92 sample shows a high TYS of 161 MPa, but its elongation is extremely low, 2.5%. All the short-aged and peak-aged GR-AZ92 samples exhibit considerably higher TYS and UTS than the homogenized commercial AZ91 sample; the TYS of the 30-min-short-aged GR-AZ92 sample is 48 MPa higher than that of the homogenized AZ91 sample, and its elongation is also higher (8.0 and 7.6% for the former and latter, respectively). As shown in Fig. 4b, the TYS and elongation of the aged GR-AZ92 samples have a logarithmic dependence on the aging time: the TYS is linearly proportional to the logarithmic aging time whereas the elongation is inversely proportional to the logarithmic aging time. This correlation between the tensile properties and the aging time indicates that the strength and ductility of the GR-AZ92 alloy can be varied by controlling the aging treatment time in order to achieve the mechanical properties required for the components used.

Figure 5 shows the TYS and elongation values of the GR-AZ92 samples as determined in this study, together with those of commercial AZ91 samples obtained from the literature [49–62]. In the as-cast state, AZ91 samples have a TYS of ~ 70–115 MPa and an elongation of ~ 2–5% [49–51, 54–61]; this difference in the strength and ductility of the same alloy is because the mechanical properties of as-cast material can be changed by tuning casting process conditions such as the size and shape of the mold, casting temperature, holding time, and cooling rate and by altering metallurgical factors such as the size and distribution of casting defects and second phases,

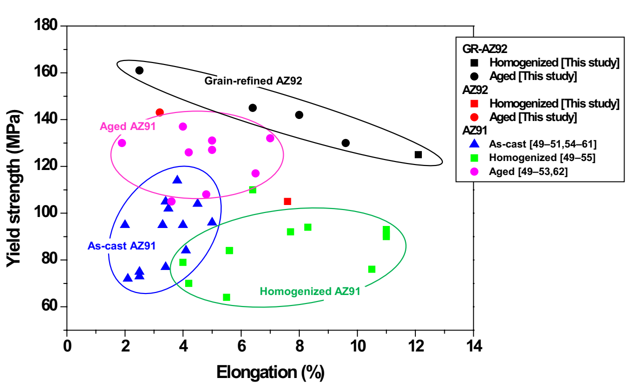

Fig. 5 Tensile yield strength and elongation of as-cast, homogenized, and/or aged AZ91, AZ92, and grain-refined AZ92 alloys

the size of grains and dendritic cells, the chemical segregation, the fluidity, the heat of fusion, and the impurity level [63]. The mechanical properties of homogenized materials also vary depending on the microstructure before homogenization, the homogenization temperature and time, the temperature of the quenching medium, the quenching delay, etc. [64]. However, a homogenized material generally exhibits a higher elongation than its as-cast counterpart owing to the microstructural stabilization of the former—e.g., a reduction in casting defects, elimination of atomic segregation, and dissolution of the second phase. The homogenized AZ91 samples also have relatively higher elongations (~ 4–11%) than the as-cast ones (~ 2–5%), but they have almost the same TYS [49–55]. In addition, when aging treatment is performed on an alloy with a supersaturated solid-solution state, its strength generally improves and its elongation decreases owing to the formation of precipitates; however, the mechanical properties of aged material are also affected by various factors such as the amount of dissolved solute atoms, their diffusivity, the aging temperature and time, the number of annealing steps, and cooling conditions [65, 66]. The TYS of the aged AZ91 samples increases to ~ 105–137 MPa by the precipitation of the $Mg_{17}Al_{12}$ phase, but their elongation decreases to the level of the as-cast AZ91 samples [49–53, 62]. The GR-AZ92 samples have higher strength and elongation than these as-cast, homogenized, and aged AZ91 samples (Fig. 5). The homogenized GR-AZ92 sample has a comparable TYS to and more than twice the elongation of the aged AZ91 samples, and the short-aged GR-AZ92 samples have higher strength and ductility than the aged AZ91 samples. The GR-AZ92 sample peak-aged for 8 h, which is shorter than the peak-aging time (~ 16–38 h) of AZ91 alloy [52, 67], shows a significantly higher strength than the aged AZ91 samples. Moreover, because the refined grains of the GR-AZ92 sample accelerate the precipitation behavior during aging, the aging time is effectively shortened; this, in turn, improves the productivity and reduces the energy used in heat treatment. Accordingly, the GR-AZ92 alloy, which has higher strength and ductility than the AZ91 alloy, can be manufactured simply by adding 1 wt% Zn and a very small amount of SiC grain refiner to the AZ91 alloy, which does not significantly increase the material cost. Moreover, since this alloy has numerous grain boundaries that serve as nucleation sites of DPs during aging, a good combination of strength and ductility with TYS larger than 130 MPa and elongation larger than 6.4% can be obtained by subjecting the alloy to a short-aging treatment less than 1 h.

4 Conclusion

With the aim of manufacturing a cast Mg alloy with superior strength and ductility, 1 wt% Zn and a very small amount of SiC (0.17 wt%) were added to commercial AZ91 alloy for enhancing the solid-solution strengthening effect and refining the crystal grains, respectively. The homogenized GR-AZ92 alloy with an average grain size of 91 μm exhibits significantly higher tensile properties (TYS of 125 MPa, UTS of 281 MPa, and elongation of 12.1%) than the homogenized AZ91 alloy (TYS of 94 MPa, UTS of 192 MPa, and elongation of 7.0%). In addition, because the refined grains accelerate the precipitation behavior induced during aging treatment, the strength of the GR-AZ92 alloy can be effectively improved, without a major reduction in its ductility, through a short-aging treatment less than 1 h. The GR-AZ92 alloy short-aged for 30 min has an excellent combination of strength and ductility, with a TYS of 142 MPa, UTS of 304 MPa, and elongation of 8.0%.

Acknowledgements This work was supported by the National Research Foundation of Korea Grant funded by the Korea government (MSIP, South Korea) (Nos. 2016R1C1B2012140 and 2017R1A4A1015628).

References

1. B.L. Mordike, T. Ebert, Mater. Sci. Eng. A **302**, 37 (2001)
2. A.A. Luo, J. Magnes, Alloys **1**, 2 (2013)
3. F. Khomamizadeh, B. Nami, S. Khoshkhooei, Metal. Mater. T. A **36A**, 3489 (2005)
4. J. Zhang, X. Niu, X. Qiu, K. Liu, C. Nan, D. Tang, J. Meng, J. Alloys Compd. **471**, 322 (2009)
5. J. Wang, L. Wang, J. An, Y. Liu, J. Mater. Eng. Perform. **17**, 725 (2008)
6. J. Zhang, D. Zhang, Z. Tian, J. Wang, K. Liu, H. Lu, D. Tang, J. Meng, Mater. Sci. Eng. A **489**, 113 (2008)
7. X. Wang, W. Du, K. Liu, Z. Wang, S. Li, J. Alloys Compd. **522**, 78 (2012)
8. K.F. Ho, M. Gupta, T.S. Srivatsan, Mater. Sci. Eng. A **369**, 302 (2004)
9. M.Y. Zheng, K. Wu, M. Liang, S. Kamado, Y. Kojima, Mater. Sci. Eng. A **372**, 66 (2004)
10. P. Poddar, V.C. Srivastava, P.K. De, K.L. Sahoo, Mater. Sci. Eng. A **460–461**, 357 (2007)
11. M. Zhen, K. Wu, C. Yao, Mater. Sci. Eng. A **318**, 50 (2001)
12. S.H. Chen, P.P. Jin, G. Schumacher, N. Wanderka, Comp. Sci. Tech. **70**, 123 (2010)
13. S.H. Park, J.H. Bae, S.H. Kim, J. Yoon, B.S. You, Metall. Mater. Trans. A **46A**, 5482 (2015)
14. A. Luo, Can. Metall. Q. **35**, 375 (1996)
15. C.L. Mendis, C.J. Bettles, M.A. Gibson, C.R. Hutchinson, Mater. Sci. Eng. A **435–436**, 163 (2006)
16. A.A. Nayeb-Hashemi, J.B. Clark, *Phase Diagrams of Binary Magnesium Alloys* (ASM International, Metals Park, 1988)
17. E.F. Emley, *Principles of Magnesium Technology* (Pergamon Press, Oxford, 1966)
18. D.H. StJohn, M. Qian, M.A. Easton, P. Cao, Z. Hildebrand, Metall. Mater. Trans. A **36A**, 1671 (2005)
19. Y.C. Lee, A.K. Dahle, D.H. StJohn, Metall. Mater. Trans. A **31**, 2895 (2000)
20. Y. Ali, D. Qiu, B. Jiang, F. Pan, M.X. Zhang, J. Alloys Compd. **619**, 639 (2015)
21. M. Qian, P. Cao, Scr. Mater. **52**, 415 (2005)
22. L. Lu, A.K. Dahle, D.H. StJohn, Scr. Mater. **53**, 517 (2005)
23. Q. Jin, J.P. Eom, S.G. Lim, W.W. Park, B.S. Lou, Scr. Mater. **49**, 1129 (2003)
24. L. Wang, Y.M. Kim, J. Lee, B.S. You, Mater. Sci. Eng. A **528**, 1485 (2011)
25. E. Yano, Y. Tamura, T. Motegi, E. Sato, J. Jpn. Inst. Light Met. **51**, 599 (2001)
26. Y.M. Kim, C.D. Yim, B.S. You, Scr. Mater. **57**, 691 (2007)
27. Y. Huang, K.U. Kainer, N. Hort, Scr. Mater. **64**, 793 (2011)
28. M.A. Easton, A. Schiffl, J.Y. Yao, H. Kaufmann, Scr. Mater. **55**, 379 (2006)
29. R. Günther, Ch. Hartig, R. Bormann, Acta Mater. **54**, 5591 (2006)
30. T.J. Chen, X.D. Jiang, Y. Ma, Y.D. Li, Y. Hao, J. Alloys Compd. **496**, 218 (2010)
31. J.G. Jung, S.H. Park, H. Yu, Y.M. Kim, Y.K. Lee, B.S. You, Scr. Mater. **93**, 8 (2014)
32. Y. Wang, M. Xia, Z. Fan, X. Zhou, G.E. Thompson, Intermetallics **18**, 1683 (2010)
33. S.H. Park, J.G. Jung, J. Yoon, B.S. You, Mater. Sci. Eng. A **626**, 128 (2015)
34. D.B. Williams, E.P. Butler, Int. Met. Rev. **26**, 153 (1981)
35. S. Celotto, Acta Mater. **48**, 1775 (2000)
36. S.-H. Kim, J.U. Lee, Y.J. Kim, J.H. Bae, B.S. You, S.H. Park, J. Mater. Sci. Technol. (2017). https://doi.org/10.1016/j.jmst.2017.11.019
37. ASM Metals Handbook, *ASM International* (Metals Park, OH, 1979)
38. C.R. Brooks, *Heat Treatment* (Structure and Properties of Nonferrous Alloys, ASM International, Metals Park, OH, 1984)
39. E. Cerri, S. Barbagallo, Mater. Lett. **56**, 716 (2002)
40. S.W. Xu, N. Matsumoto, S. Kamado, T. Honma, T. Kojima, Mater. Sci. Eng. A **523**, 47 (2009)
41. D. Zhao, Z. Wang, M. Zuo, H. Geng, Mater. Des. **56**, 589 (2014)
42. S. Jayalakshmi, S.V. Kailas, S. Seshan, Comp. A Appl. Sci. Manuf. **33**, 1135 (2002)
43. Y. Wang, G. Liu, Z. Fan, Scr. Mater. **54**, 903 (2006)
44. Z.M. Li, A.A. Luo, Q.G. Wang, L.M. Peng, P.H. Fu, G.H. Wu, Mater. Sci. Eng. A **564**, 450 (2013)
45. T.M. Yue, H.U. Ha, N.J. Musson, J. Mater. Sci. **30**, 2277 (1995)
46. M.H. Yoo, Metall. Trans. A **12**, 409 (1981)
47. A. Jain, O. Duygulu, D.W. Brown, C.N. Tome, S.R. Agnew, Mater. Sci. Eng. A **486**, 545 (2008)
48. A. Ghaderi, M.R. Barnett, Acta Mater. **59**, 7824 (2011)
49. S.S. Park, Y.S. Park, N.J. Kim, Met. Mater. Int. **8**, 551 (2002)
50. H. Hu, J. Mater. Sci. **33**, 1579 (1998)
51. M. Suresh, A. Srinivasan, U.T.S. Pillai, B.C. Pai, Mater. Sci. Eng. A **528**, 8573 (2011)
52. X.J. Wang, X.S. Hu, W.Q. Liu, J.F. Du, K. Wu, Y.D. Huang, M.Y. Zheng, Mater. Sci. Eng. A **682**, 491 (2017)
53. C.H. Cáceres, C.J. Davidson, J.R. Griffiths, C.L. Newton, Mater. Sci. Eng. A **325**, 344 (2002)
54. S. Kleiner, O. Beffort, A. Wahlen, P.J. Uggowitzer, J. Light Met. **2**, 277 (2002)
55. K.B. Nie, X.J. Wang, K. Wu, M.Y. Zheng, X.S. Hu, Mater. Sci. Eng. A **528**, 7484 (2011)
56. A.H. Feng, B.L. Xiao, Z.Y. Ma, R.S. Chen, Metall. Mater. Trans. A **40**, 2447 (2009)
57. M. Suresh, A. Srinivasan, K.R. Ravi, U.T.S. Pillai, B.C. Pai, Mater. Sci. Eng. A **525**, 207 (2009)
58. A.H. Feng, Z.Y. Ma, Scr. Mater. **56**, 397 (2007)
59. Y. Turen, Mater. Des. **49**, 1009 (2013)
60. D.R. Ni, D. Wang, A.H. Feng, G. Yao, Z.Y. Ma, Scr. Mater. **61**, 568 (2009)
61. S. Candan, M. Unal, M. Turkmen, E. Koc, Y. Turen, E. Candan, Mater. Sci. Eng. A **501**, 115 (2009)
62. X. Feng, M. Xuegang, S. Yangshan, J. Mater. Sci. **41**, 4725 (2006)

63. R.W. Heine, C.R. Loper Jr., P.C. Rosenthal, *Principles of Metal Casting*, 2nd edn. (McGraw-Hill Book Company, New York, 1967)
64. W.D. Callister Jr., D.G. Rethwisch, *Fundamentals of Materials Science and Engineering*, 3rd edn. (Wiley, New York, 2007)
65. P. Monica, P.M. Bravo, D. Cardenas, J. Mater. Proc. Tech. **239**, 297 (2017)
66. Q.Z. Peng, H.T. Zhou, F.H. Zhong, H.B. Ding, X. Zhou, R.R. Liu, T. Xie, Y. Peng, Mater. Des. **66**, 566 (2015)
67. J.K. Kim, S.H. Oh, K.C. Kim, W.T. Kim, D.H. Kim, Met. Mater. Int. **23**, 308 (2017)